Electronic Supplementary Material (ESI) for Soft Matter


# Supplementary Information

## Highly Ordered Superstructures of Single Wall Carbon Nanotube-Liposome Complexes

*Tae-Hwan Kim, Changwoo Doe, Shin-Hyun Kang, Min-Jae Lee, Sung-Hwan Lim, and Sung-Min Choi**

### Preparation of *p*-SWNT25

HiPco single wall carbon nanotubes (SWNTs, 2 mg/mL) were mixed with cetyltrimethylammonium 4-vinylbenzoate (CTVB, 5 mg/mL) containing a polymerizable counterion and sodium styrenesulfonate (NaSS) 25 mol % (relative to the CTVB concentration) in heavy water ($D_2O$) and then sonicated (Cole-Parmer VCX750, 20 kHz, 750 W) for 1 hour at 60 °C. After sonication, the counterions of the CTVB were polymerized using the VA-044 free radical initiator at 60 °C. To separate the individually isolated SWNTs, the suspension was ultracentrifuged at ca. 111,000g for 4 hours (Beckman XL-100) and the upper ca. 70 % of the solution was decanted. From the UV-vis-NIR absorbance at 744 nm, the concentration of SWNT (0.07 mg/mL) in the decanted *p*-SWNT25 dispersions was estimated by Beer's law[1]. The concentration of CTVB/NaSS surfactant (1.847 mg/mL) was calculated from thermogravimetric analysis (TGA) and the SWNT concentration estimated from the UV-vis-NIR measurement. The decanted *p*-SWNT25 dispersion in water was freeze-dried at -55 °C for 3 days, resulting in a black powder of *p*-SWNT25.

## $^1$H-NMR measurement of *p*-SWNT25

To characterize the degree of polymerization of CTVB and NaSS molecules for *p*-SWNT25, a series of $^1$H NMR measurements (Bruker FT-500 MHz NMR spectrometer) were performed for the unpolymerized and polymerized SWNT/CTVB/NaSS in $D_2O$. The $^1$H NMR spectrum of the unpolymerized SWNT/CTVB/NaSS is shown in Fig. S1a. The peaks correspond to the protons in the alkyl chain group (1.0 and 1.39 ppm), the 3 methyl groups coupled with nitrogen (2.93 ppm), residual $H_2O$ (4.8 ppm), the vinyl group (5.17, 5.72, and 6.60 ppm), and the aromatic group (7.25 and 7.83 ppm). Since the counterion ($SS^-$) of NaSS molecules is composed of the same aromatic and vinyl groups as that ($VB^-$) of CTVB molecules, the spectrum of the unpolymerized SWNT/CTVB/NaSS mixture is very similar to that of unpolymerized SWNT/CTVB mixture[1]. The $^1$H-NMR spectrum of the polymerized SWNT/CTVB/NaSS (*p*-SWNT25) is shown in Fig. S1b. It should be noted the peaks arising from the vinyl and aromatic groups of the polymerizable counterions ($VB^-$ and $SS^-$ ions) almost completely disappear upon polymerization. This disappearance of peaks is due to the reduced mobility of $VB^-$ and $SS^-$ ions upon their polymerization and hence shortened T2-relaxtion time. This clearly indicates that almost all of $VB^-$ and $SS^-$ ions are polymerized, forming stable *p*-SWNT25.

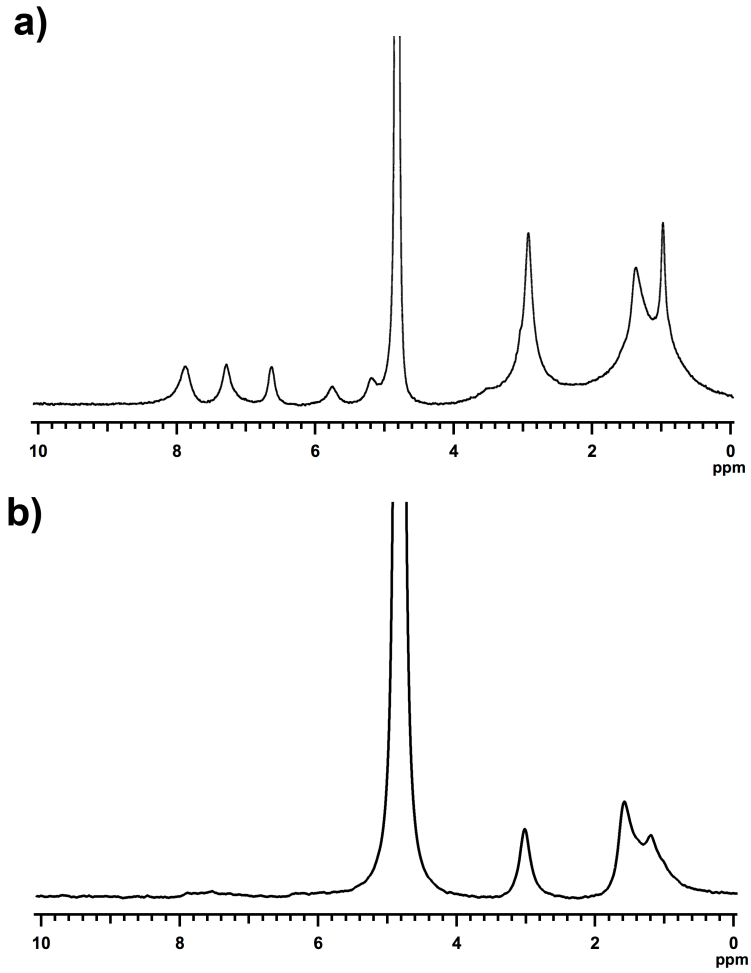


**Fig. S1** $^{1}$H-NMR spectra of a) unpolymerized SWNT/CTVB/NaSS and b) *p*-SWNT25 in $D_2O$.

## UV-vis-NIR spectra of *p*-SWNT25 after and before freeze drying

The UV-vis-NIR spectra of the *p*-SWNT25 dispersion in water showed a sharp van Hove transition, which is typical for individually isolated SWNT in solution[2-7] (Fig. S2). The freeze-dried *p*-SWNT25 was easily re-dispersible in water with mild vortexing for a few minutes without forming any visible aggregates. The UV-vis-NIR spectrum of *p*-SWNT25 dispersion as prepared and that of re-dispersed *p*-SWNT25 after freeze drying were essentially identical (Fig. S2), indicating the excellent re-dispersibility of *p*-SWNT25.

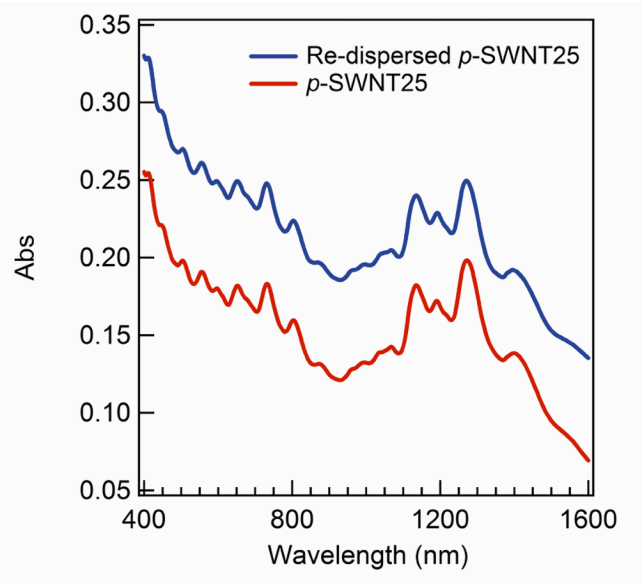


**Fig. S2** UV-vis-NIR spectra of *p*-SWNT25 before and after freeze drying. The spectrum of the re-dispersed *p*-SWNT25 is shifted vertically for visual clarity.

## Determination of the isoelectric points of *p*-SWNT25-CL complexes

The zeta potentials of *p*-SWNT25-cationic liposome (CL) complexes ($\Phi_{DOPE}$ = 0.33, 0.5, 0.67, 0.75, 0.8, and 0.85) for various CL/*p*-SWNT25 mass ratios (L/S) were measured. As the L/S mass ratio increases, the zeta potential changes its sign from negative to positive, from which the isoelectric points of *p*-SWNT25-CL complexes are determined, as indicated by blue dotted lines in Fig. S3. The dynamic light scattering measurements of the *p*-SWNT25-CL complexes show that they form large aggregates at the isoelectric points (Fig. S4).

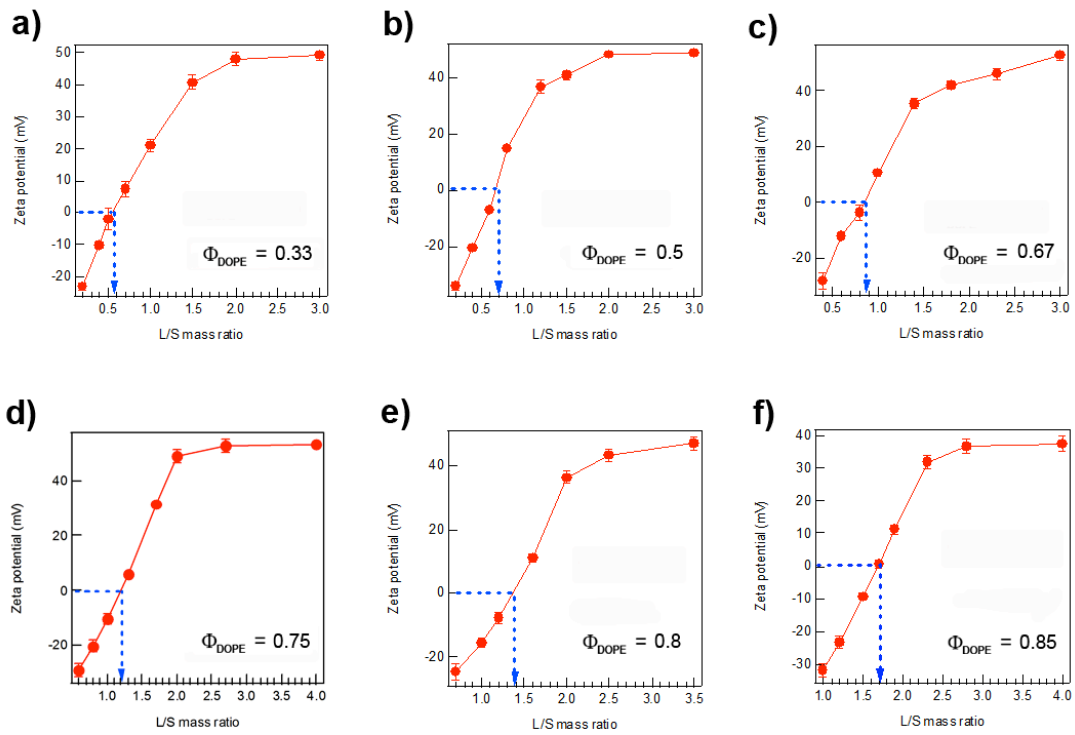


**Fig. S3** Zeta potentials of *p*-SWNT25-CL complexes at various L/S mass ratios. $\Phi_{DOPE}$ = a) 0.33, b) 0.5, c) 0.67, d) 0.75, e) 0.8, and f) 0.85.

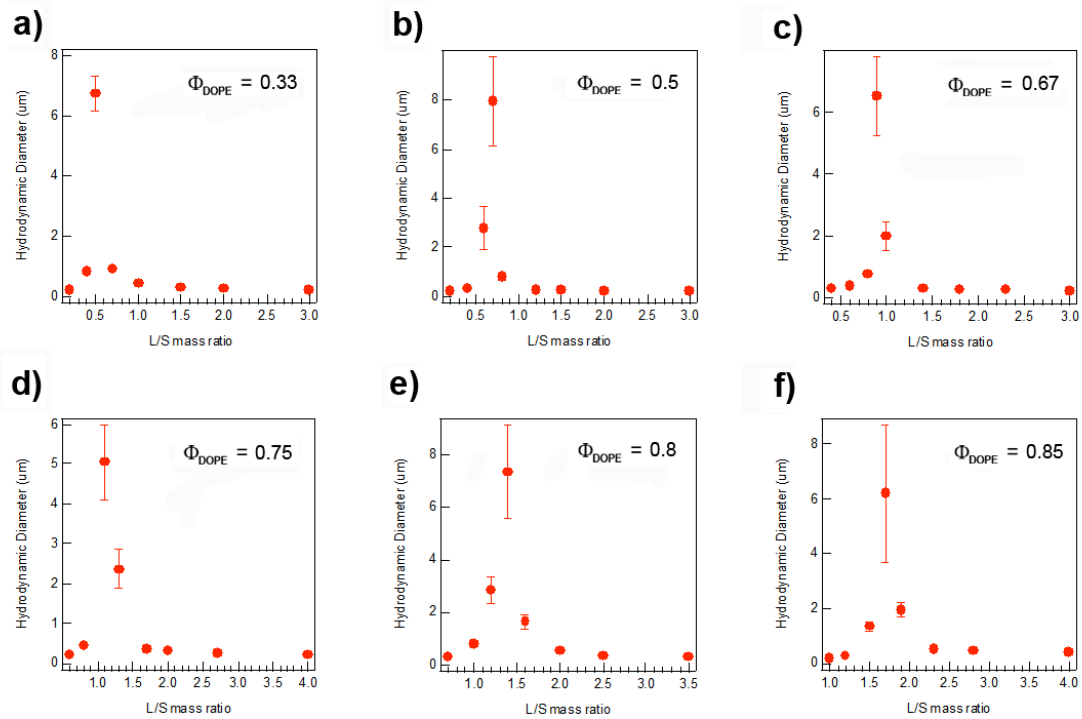


**Fig. S4** Hydrodynamic diameters of *p*-SWNT25-CL complexes at various L/S mass ratios. $\Phi_{DOPE}$ = a) 0.33, b) 0.5, c) 0.67, d) 0.75, e) 0.8, and f) 0.85.

## Structure of *p*-SWNT25

The structure of *p*-SWNT25 was confirmed by atomic force microscopy (AFM) measurements as shown in Fig. S5. The diameter distribution of bare SWNTs (which are obtained by burning the *p*-SWNT25 for 4 hr at 330 °C to remove CTVB/NaSS layer absorbed on SWNT) is peaked at (1 ± 0.1) nm, and diameters less than 2 nm occupy 90% of the distribution, which indicates that *p*-SWNT25s are dispersed in an isolated form or in a very small bundle (Fig. S5a). The diameter distribution of *p*-SWNT25s is peaked at (5 ± 0.1) nm, and 87% of the distribution is in the range of 4.4–5.6 nm (Fig. S5b). The polymerized surfactant shell thickness of the *p*-SWNT25s, which is determined from the diameter distributions of bare SWNT (ca. 1 nm) and *p*-SWNT25 (ca. 5 nm), is about 2 nm. The length distribution of the *p*-SWNT25 is peaked at (500 ± 50) nm with a mean length of ca. 500 nm (Fig. S5c). This result is consistent with the AFM result of *p*-SWNTs[1] (functionalized SWNTs fabricated in the exactly same procedure as *p*-SWNT25, except that NaSS was not added.).

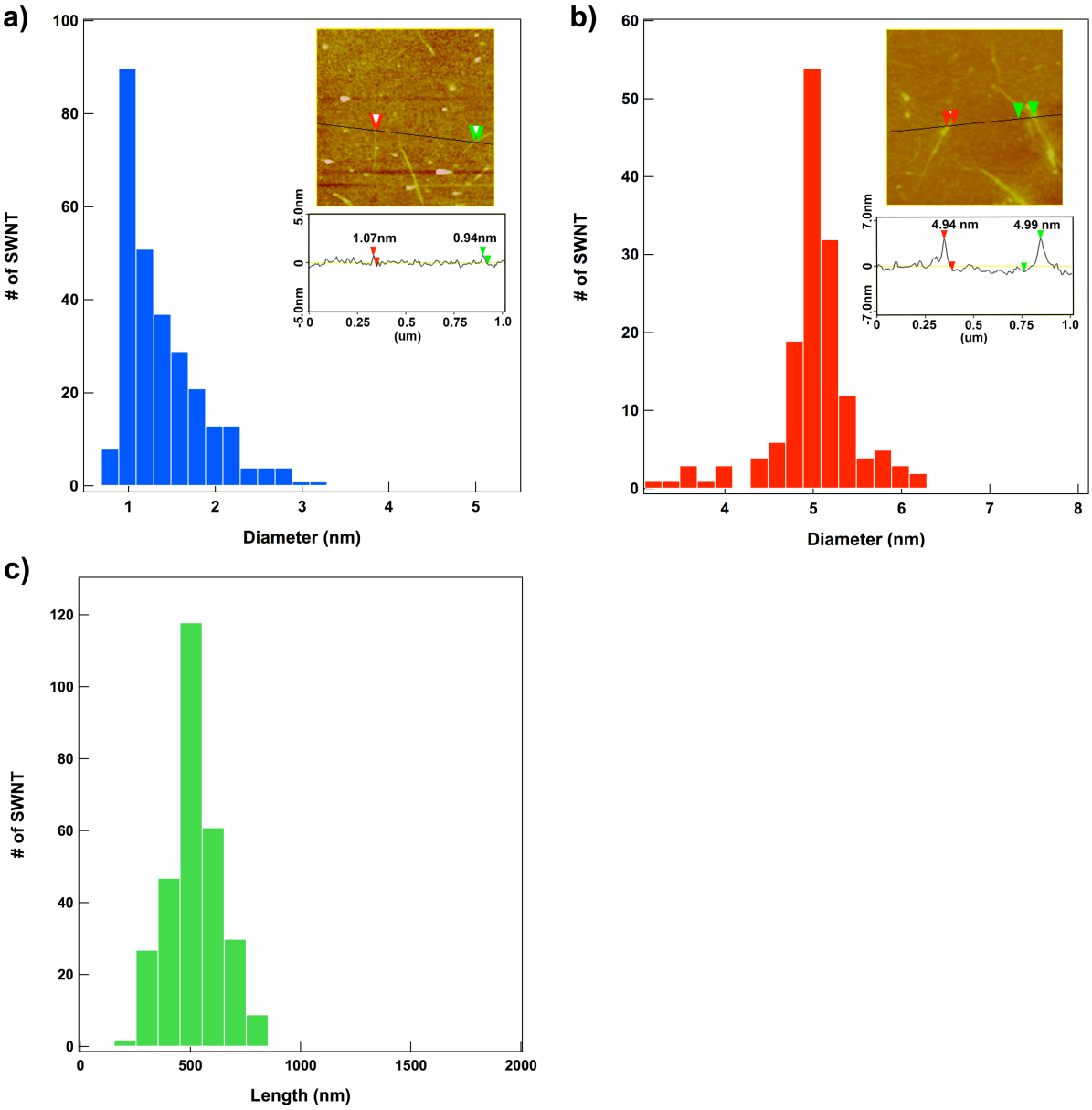


**Fig. S5** The diameter distributions of a) the bare SWNTs and b) *p*-SWNT25s. c) The length distribution of *p*-SWNT25s. The insets are AFM images (1 $\mu$m×1 $\mu$m) and sectional analyses of a) bare SWNTs and b) *p*-SWNT25s.

**Reference**


1 T.-H. Kim, C. Doe, S. R. Kline, S.-M. Choi, *Adv. Mater.* 2007, **19**, 929.

2 M. J. O'Connell, S. M. Bachilo, C. B. Huffman, V. C. Moore, M. S. Strano, E. H. Haroz, K. L. Rialon, P. J. Boul, W. H. Noon, C. Kittrell, J. Ma, R. H. Hauge, R. B. Weisman, R. E. Smalley, *Science* 2002, **297**, 593.

3 A. M. Rao, E. Richter, S. Bandow, B. Chase, P. C. Eklund, K. A. Williams, S. Fang, K. R. Subbaswamy, M. Menon, A. Thess, R. E. Smalley, G. Dresselhaus, M. S. Dresselhaus, *Science* 1997, **275**, 187.

4 X. Zhang, T. Liu, T. V. Sreekumar, S. Kumar, V. C. Moore, R. H. Hauge, R. E. Smalley, *Nano Lett.* 2003, **3**, 1285.

5 V. C. Moore, M. S. Strano, E. H. Haroz, R. H. Hauge, R. E. Smalley, *Nano Lett*. 2003, **3**, 1379.

6 A. G. Ryabenko, T. V. Dorofeeva, G. I. Zvereva, *Carbon* 2004, **42**, 1523.

7 A. Di Crescezo, D. Demurtas, A. Renzetti, G. Siani, P. De Maria, M. Meneghetti, M. Prato, A. Fontana, *Soft Matter* 2009, **5**, 62.